Macromolecules

Article

pubs.acs.org/Macromolecules

Construction and Properties of Hyperbranched Block Copolymer with Independently Adjustable Heterosubchains

Jinxian Yang,[†] Lianwei Li,*[,†] Zongyang Jing,[†] Xiaodong Ye,*[,†] and Chi Wu[†,‡]

[†]Hefei National Laboratory for Physical Sciences at the Microscale, Department of Chemical Physics, University of Science and Technology of China, Hefei, Anhui 230026, China

[‡]Department of Chemistry, The Chinese University of Hong Kong, Shatin N.T., Hong Kong

Supporting Information

ABSTRACT: A trifunctional initiator with one alkyne, one hydroxyl, and one bromine group was used to construct Br-polystyrene-alkyne-poly(ε-caprolactone)-OH (Br−PS−≡−PCL−OH) diblock copolymer precursor with one terminal alkyne group located at the junction between the two blocks. Further bromination and azidation substitution of the precursor led to a seesaw-type macromonomer azide-polystyrene-alkyne-poly(ε-caprolactone)-azide (N_3−PS−≡−PCL−N_3). Subsequently, novel hyperbranched copolymers [HB-(PS-*b*-PCL)$_n$] with independently adjustable PS and PCL branching subchains were prepared by "click" chemistry. All of the linear precursors and hyperbranched copolymers were characterized by FT-IR, ^{1}H NMR, and GPC with triple detectors in detail. It was found that such hyperbranched copolymers are self-similar objects; namely, their intrinsic viscosities ([η]) are scaled to the weight-average molar masses (M_w) as [η] ~ M_w^{ν}, where ν = 0.45 ± 0.01 and 0.48 ± 0.01 for the longer and shorter PS block, respectively. Moreover, the study on the crystallization behavior of unfractionated and fractionated HB-(PS-*b*-PCL)$_n$ copolymers indicated both the crystal size and the degree of crystallinity decrease with the PS subchain length and the overall degree of polymerization, and the remaining oligomer and macromonomer components could facilitate the crystallization of the unfractionated sample. Finally, it was found that the degree of crystallinity decreases dramatically when the weight fraction of fractionated hyperbranched copolymer in macromonomer/hyperbranched copolymer blend films exceeds ~67%, indicating that the uncrystallizable hyperbranched chains may impose some extra restriction on the crystallization of the macromonomer chains.

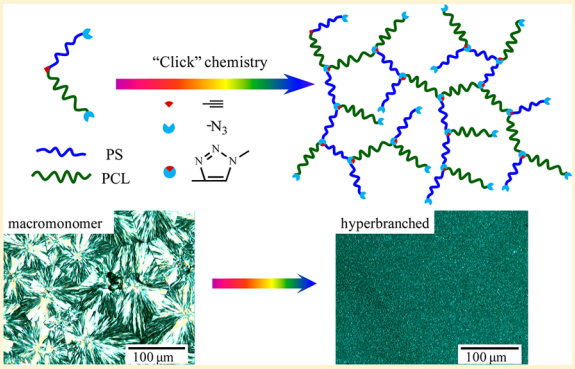

INTRODUCTION

Hyperbranched polymers with well-defined long subchains have recently attracted interest due to their unique bulk and solution properties in comparison with hyperbranched polymers with short and rigid subchains,[1−10] such as much higher mechanical strength and different phase morphologies in bulk[3−5] as well as more interesting rheological property[3,11] and self-assembled structures in solution.[7,10] Thus, plentiful research work has been devoted to investigating the structure−property correlation of long subchain hyperbranched polymers. Namely, Hedrick et al. developed a method using AB_2-type macromonomers with short polymer subchains to synthesize hyperbranched PCL and studied their properties;[12−16] recently, Hutching et al.[5] synthesized complex hyperbranched (co)-polymer architectures by using AB_2-type polyisoprene and polystyrene as macromonomers and investigated their solid-state morphologies and mechanical properties. However, conventional A_2 + B_3 or Y-type AB_2 approaches always lead to broadly distributed lengths of the subchains between any two neighboring branching points,[3,4,9,17−20] which has hindered the quantitative study of their structure−property correlation.

Previously, using a recently developed B~~A~~B seesaw-type macromonomer strategy, we prepared different kinds of hyperbranched (co)polymers with uniform subchains, where A and B represent alkyne and azide groups, respectively, and ~~ represents a polymer block.[21−24] The scaling relations between their sizes (R), intrinsic viscosities ([η]), and molar masses (M) were evaluated;[25] how these hyperbranched chains pass through a small cylindrical pore was studied;[26] and their intrachain folding and interchain association in dilute and semidilute solutions were explored.[10] More recently, Kawaguchi et al.[27] also used a similar approach to prepare a series of hyperbranched poly(L-lactide)s (PLA) and studied how the branching density affects the crystallization of hyperbranched PLA chains.

Those previously studied long-subchain hyperbranched polymers were prepared solely by using either living radical polymerization of vinyl monomers,[21−23,25,26,28−30] such as styrene, methyl methacrylate, and *tert*-butyl acrylate, or ring-opening

Received: September 22, 2014
Revised: October 31, 2014
Published: November 17, 2014

polymerization (ROP) of cyclic monomers, such as ε-caprolactone[12] and lactide.[27] In contrast, a combination of these two methods can extremely expand the category of hyperbranched copolymers made of two different types of monomers; on the other hand, hyperbranched copolymers containing two different branching subchains with controllable lengths own their unique applications in various fields, including the self-assembled nanostructures,[31−34] emulsion stabilizers,[35] and drug carriers.[36−38] It is well-known that the copolymers with a linear diblock or triblock structure are assumed to have fewer certain advantages compared to their hyperbranched counterpart, such as the formation of small unimolecular micelles,[31,39] lower viscosity, and less entanglement.[40,41] However, the construction of a hyperbranched structure which simultaneously contains vinyl and cyclic comonomers has not been reported so far.

In this paper, we report a newly developed approach to construct hyperbranched copolymers with two independently adjustable branching subchains; more specifically, a B∼∼A---B seesaw-type diblock was constructed as macromonomer precursor, where ∼∼ and --- represent different polymer blocks. Here, we chose styrene (vinyl monomer) and ε-caprolactone (cyclic monomer) as two kinds of model monomers to construct model hyperbranched copolymers with two kinds of controllable uniform long subchains (Scheme 1).

Scheme 1. Schematic of Synthesis of Seesaw-Type Diblock Macromonomer $N_3–PS–PCL–N_3$

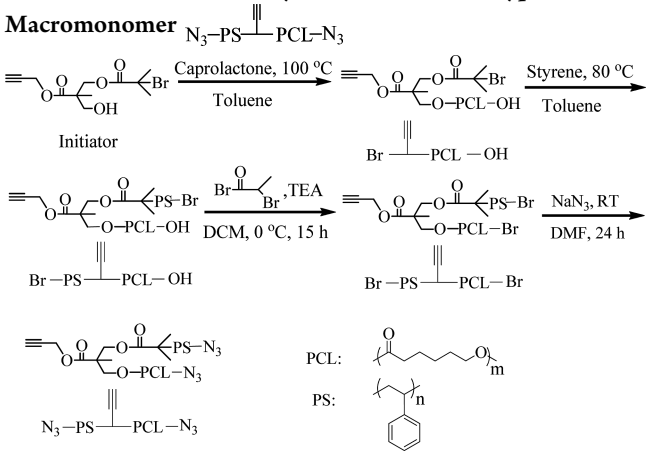

To prepare B∼∼A---B, we started with a trifunctional initiator with one alkyne (≡), one hydroxyl (OH), and one bromine group (Br) to first initiate the polymerization of ε-caprolactone and then the polymerization of styrene by successive ring-opening polymerization (ROP) and atom transfer radical polymerization (ATRP), resulting in two diblock macromonomers ($Br–PS–PCL–OH$) with an identical PCL block but two PS blocks with different lengths. Further bromination and azidation led to two $N_3–PS–PCL–N_3$ precursors. Finally, using an effective interchain azide−alkyne cycloaddition "click" reaction,[42−44] we interconnected each kind of $N_3–PS–PCL–N_3$ precursor chains together to form a hyperbranched copolymer [HB-(PS-*b*-PCL)$_n$] with two different kinds of subchains, but each subchain has a controllable and uniform length. The precursors and the resultant hyperbranched copolymers were characterized by Fourier transform infrared (FT-IR) spectroscopy, proton nuclear magnetic resonance (^{1}H NMR), and gel permeation chromatography (GPC) equipped with triple detectors: refractive index (RI), multiangle-laser-light-scattering (MALLS), and viscosity detectors. Finally, by using the polarizing optical microscopy (POM) and differential scanning calorimetry (DSC), the effects of the PS subchain length, the overall molar mass, and the polydispersity of hyperbranched copolymers on their crystallization properties were investigated; more in depth, the crystallization property of polymer blends of one narrowly distributed HB-(PS-*b*-PCL)$_n$ fraction and its linear precursor was explored.

EXPERIMENTAL SECTION

Materials. Styrene (St, Sinopharm, 97%) was first passed through a basic alumina column and then distilled under a reduced pressure over calcium hydride (CaH_2). ε-Caprolactone (CL, Aladdin, 99%) was dried over CaH_2 and distilled under a reduced pressure. Copper(I) bromide (CuBr, Alfa Aesar, 98%) was washed with glacial acetic acid to remove soluble oxidized species, filtrated, washed with ethanol, and dried under vacuum. Dimethylformamide (DMF, Sinopharm, 97%) was first dried with anhydrous magnesium sulfate ($MgSO_4$) and then distilled under a reduced pressure. Toluene (Sinopharm, 97%) was refluxed over sodium for 24 h and then distilled. Dichloromethane (DCM, Sinopharm, 97%) and triethylamine (TEA, Sinopharm, 97%) were distilled over CaH_2. Sodium azide (NaN_3, Aldrich, 99%), tris(2-(dimethylamino)ethyl)amine (Me_6TREN, Alfa Aesar, 98%), *N*,*N*,*N*′,*N*′,*N*″-pentamethyldiethylenetriamine (PMDETA, Aldrich, 99%), tin(II) 2-ethylhexanoate ($Sn(EH)_2$, Aldrich, 95%), and other analytical grade reagents from Sinopharm were used as received.

Characterization. *Proton Nuclear Magnetic Resonance Spectroscopy (^{1}H NMR).* ^{1}H NMR measurements were conducted on a Bruker AV400 NMR spectrometer using deuterated chloroform ($CDCl_3$) as solvent and tetramethylsilane (TMS) as an internal standard. The polymer solutions had a concentration of ∼20 g/L.

Fourier Transform Infrared (FT-IR) Spectroscopy. FT-IR spectra were performed on a Bruker VECTOR-22 IR spectrometer. The spectra of all samples were collected at 64 scans with a spectral resolution of 4 cm^{-1} by the KBr disk method.

Gel Permeation Chromatography (GPC) with Triple Detectors. The relative number- and weight-average molar masses ($M_{n,RI}$ and $M_{w,RI}$), the absolute number- and weight-average molar masses ($M_{n,MALLS}$ and $M_{w,MALLS}$), and the intrinsic viscosity ([η]) were determined at 35 °C by gel permeation chromatography (GPC, Waters 1515) equipped with three Waters Styragel columns (guard, HR 0.5, HR 1, and HR 4), a Waters 717 PLUS autosampler, a Waters 2414 differential refractometer, a multiangle-laser-light-scattering (MALLS) detector, and a Wyatt ViscoStar viscometer. Tetrahydrofuran (THF) was used as the eluent at a flow rate of 1.0 mL/min. The specific refractive index increments (d*n*/d*C*) of HB-(PS-*b*-PCL)$_n$ copolymers in THF were estimated from the additive rule:

$$dn/dC = W_{PS}(dn/dC)_{PS} + W_{PCL}(dn/dC)_{PCL} \quad (1)$$

where W_{PS} and W_{PCL} are the weight fractions of PS and PCL and $(dn/dC)_{PS}$ and $(dn/dC)_{PCL}$ in THF are 0.185 and 0.06 mL/g, respectively.

Differential Scanning Calorimetry (DSC). DSC was performed on a Q2000 differential scanning calorimetry from TA Instruments under a nitrogen flow rate of 100 mL/min. The samples were prepared by dropping the polymer THF solution onto glass slides and followed by evaporation at room temperature for 24 h. First, the sample was heated from −90 to 150 °C to remove the thermal history, and then the sample was reheated after cooling down from 150 to −90 °C at a scanning rate of 10 °C/min. The exothermic and the endothermic maximum temperatures were taken as the crystallization temperature (T_c) and the melting temperature (T_m), respectively. The degree of crystallinity (χ_c) is calculated according to the equation[45,46]

$$\chi_c = \Delta H_m/(W_{PCL}\Delta H_{m,0}) \quad (2)$$

where ΔH_m is the heat of fusion per gram of copolymers determined based on the endothermic peak. $\Delta H_{m,0}$ = 136.4 J/g is the heat of

dx.doi.org/10.1021/ma501948g | Macromolecules 2014, 47, 8437−8445

fusion of 100% crystalline PCL.[5] W_{PCL} is the weight fraction of PCL in the copolymer which was calculated by ^{1}H NMR integral.

Polarizing Optical Microscopy (POM). The polarizing optical microscopy images were taken by Olympus polarizing microscope with BX51 F system. Each film was prepared by dropping the polymer THF solution with a concentration of 30 mg/mL onto a glass slide and followed by evaporation at room temperature for 24 h.

Preparation of Br–(≡)–PCL–OH by Ring-Opening Polymerization (ROP). 0.72 g of initiator (2.2 mmol), 7.72 g of ε-caprolactone (67.7 mmol), and 0.18 g of $Sn(EH)_2$ (0.4 mmol) were added into a 100 mL three-neck bottle, and then 40 mL of anhydrous toluene was added. The mixture was stirred for 5 h at 100 °C under an argon atmosphere. Then the solvent was removed by rotary evaporation, and the product was redissolved in THF. The polymer solution was precipitated into an excess of the mixture of cold methanol/water (3/1, v/v). White solid Br–(≡)–PCL–OH (yield: 7.4 g, 90%) was obtained after drying under vacuum for 24 h.

Preparation of Br–PS–(≡)–PCL–OH by Atom Transfer Radical Polymerization (ATRP). 1.0 g of Br–(≡)–PCL–OH (0.33 mmol), 3.46 g of St (33.6 mmol), 31 mg of Me_6TREN (0.13 mmol), 54 mg of $Sn(EH)_2$ (0.13 mmol), and 2 mL of anhydrous toluene were added into a 15 mL glass tube with a magnetic stirrer. After degassed by three freeze–vacuum–thaw cycles, 5 mg of CuBr (0.033 mmol) was added into the tube with a hot funnel, and then the tube was sealed under vacuum. The mixture was stirred for 1.5 h (or 0.5 h to get smaller PS block) at 80 °C in a water bath. Then the tube was rapidly cooled to room temperature. The mixture was diluted with THF and passed through a short neutral alumina column to remove the metal salt. After removing all the solvents by rotary evaporator, the residue was dissolved in THF and precipitated into an excess amount of cold methanol/water mixture (3/1, v/v). White solid Br–PS–(≡)–PCL–OH (yield: 2.1 g, 88%) was obtained after drying under vacuum for 24 h.

Preparation of Br–PS–(≡)–PCL–Br by Bromination Reaction. 1.4 g of Br–PS–(≡)–PCL–OH (0.2 mmol), 0.30 g of TEA (3 mmol), and 15 mL of anhydrous DCM were added into a 50 mL three-neck bottle. 2-Bromopropiomyl bromide (0.63 g, 3 mmol) dissolved in 5 mL of anhydrous DCM was added dropwise with a constant pressure funnel in 1 h at 0 °C. After 24 h, the solvent was removed. The residue was redissolved in THF. After the removal of insoluble salts by filtration, the filtrate was concentrated by a rotary evaporator. The polymer was precipitated into an excess amount of cold methanol/water mixture (3/1, v/v). Light yellow solid Br–PS–(≡)–PCL–Br (yield: 1.2 g, 85%) was obtained after drying under vacuum for 24 h.

Preparation of N_3–PS–(≡)–PCL–N_3 by Azidation. 1.0 g of Br–PS–(≡)–PCL–Br (0.14 mmol) and 0.2 g of NaN_3 (3.1 mmol) were added into a 50 mL three-neck bottle, and then 18 mL of anhydrous DMF was added. The mixture was stirred for 24 h under an argon atmosphere at room temperature. Then the solvent was removed by rotary evaporation, and the product was redissolved in THF. The polymer solution was precipitated into an excess amount of cold methanol/water mixture (3/1, v/v) after centrifugation. The product N_3–PS–(≡)–PCL–N_3 (yield: 0.85 g, 86%) was light yellow power after drying under vacuum overnight.

Preparation of HB-(PS-b-PCL)$_n$ by "Click" Reaction. As shown in Scheme 2, 0.1 g of N_3–PS–(≡)–PCL–N_3 (0.014 mmol), 15 μL of PMDETA (0.069 mmol), and 0.5 mL of DMF were added into a 2 mL glass tube with a magnetic stirrer. 10 mg of CuBr (0.069 mmol) was added into the tube immediately with a hot funnel after degassed by three freeze–vacuum–thaw cycles, and then the tube was sealed under vacuum. The mixture was stirred for 24 h at 60 °C in water bath. After that, the tube was rapidly cooled to room temperature. The mixture was diluted with THF and passed through a short neutral alumina column to remove the metal salt. After removing all the solvents by rotary evaporator, the residue was redissolved in THF and precipitated into an excess of the mixture of cold methanol/water (3/1, v/v). White solid HB-(PS-*b*-PCL)$_n$ (yield: 68 mg, 68%) was obtained after drying under vacuum for 24 h.

Scheme 2. Schematic of Topological Structure of HB-(PS-*b*-PCL)$_n$ Prepared via Self-Polycondensation

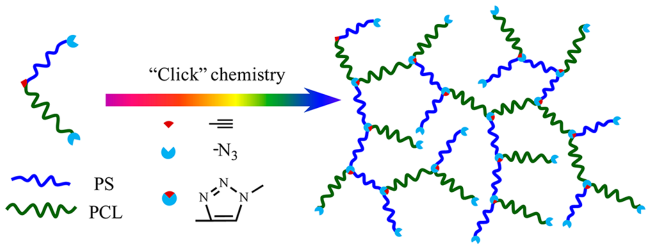

RESULTS AND DISCUSSION

The preparation of the trifunctional initiator can be found elsewhere.[47] The purity of the initiator was confirmed by ^{1}H NMR, as shown in Figure 1. Using this initiator, we successively obtained precursors Br–(≡)–PCL–OH and Br–PS–(≡)–PCL–OH by ROP of ε-caprolactone and ATRP of styrene. The absolute degrees of polymerization (DP) of PCL and PS blocks were determined by ^{1}H NMR. Figure 2 shows that the characteristic peaks located at ~4.00 ppm ("d") and ~3.65 ppm ("d′") are attributed to the protons of $-CH_2OOC-$ and $-CH_2-OH$ on the chain backbone and end of each PCL block, respectively. Therefore, DP of the PCL block was calculated according to the area ratio (A) of the two peaks as

$$DP_{PCL} = (A_d + A_{d'})/A_{d'} \quad (3)$$

Similarly, we calculated the DP of the PS block according to the area ratio of the peak (a) and peaks (d and d′) as

$$DP_{PS} = (2DP_{PCL}A_a)/(5(A_d + A_{d'})) \quad (4)$$

For the sake of convenience, the PCL homopolymers and the PCL-*b*-PS diblock copolymers with different block lengths of PCL and PS are denoted hereafter as Br–(≡)–PCL$_n$–OH and Br–PS$_m$–(≡)–PCL$_n$–OH, where n and m are the DP of PCL and PS determined by ^{1}H NMR spectroscopy, respectively.

Further conversion of precursor Br–PS$_{39}$–(≡)–PCL$_{28}$–OH into Br–PS$_{39}$–(≡)–PCL$_{28}$–Br in a 15-fold excess amount of bromination agent, 2-bromopropionyl bromide, with respect to the hydroxyl

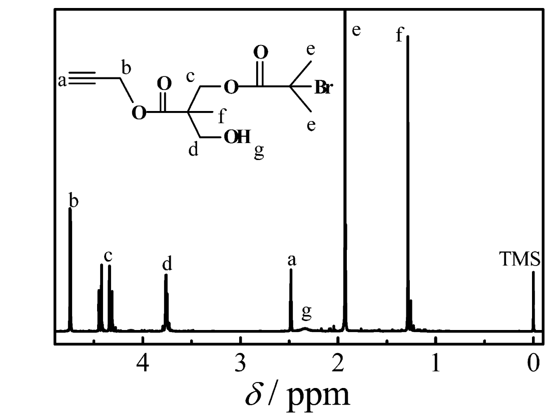

Figure 1. ^{1}H NMR spectrum of the trifunctional initiator.

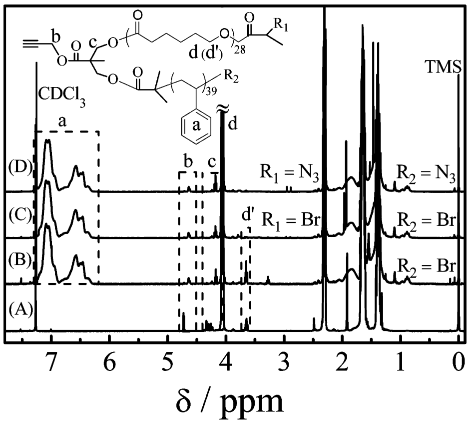

Figure 2. ^{1}H NMR spectra of (A) $\mathrm{Br{-}\overset{\equiv}{\bot}{-}PCL_{28}{-}OH}$, (B) $\mathrm{Br{-}PS_{39}{-}\overset{\equiv}{\bot}{-}PCL_{28}{-}OH}$, (C) $\mathrm{Br{-}PS_{39}{-}\overset{\equiv}{\bot}{-}PCL_{28}{-}Br}$, and (D) $\mathrm{N_3{-}PS_{39}{-}\overset{\equiv}{\bot}{-}PCL_{28}{-}N_3}$.

groups is reflected in the disappearance of the proton signals (~3.65 ppm, "d′" in Figure 2) of the $-CH_2-OH$ located at the end of the PCL block. The substitution extent was evaluated to be over 95%. Note that both of the bromine atoms located at the PS and PCL block ends are bonded to secondary carbon atoms, which avoided the possible reactivity difference between the two bromine atoms.

The GPC curves of the prepared linear chain precursors are shown in Figure 3. The polydispersity index (M_w/M_n) of the

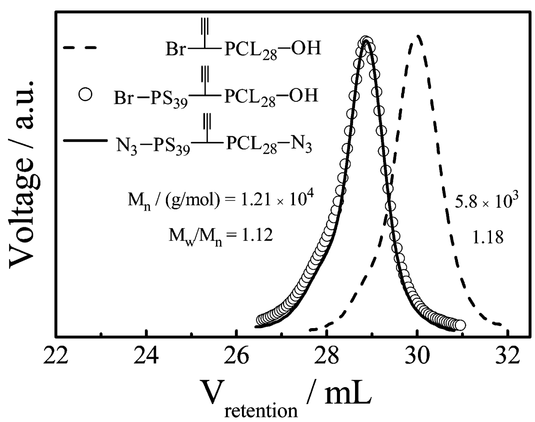

Figure 3. GPC curves of the linear chain precursors $\mathrm{Br{-}\overset{\equiv}{\bot}{-}PCL_{28}{-}OH}$, $\mathrm{Br{-}PS_{39}{-}\overset{\equiv}{\bot}{-}PCL_{28}{-}OH}$, and $\mathrm{N_3{-}PS_{39}{-}\overset{\equiv}{\bot}{-}PCL_{28}{-}N_3}$.

first block $\mathrm{Br{-}\overset{\equiv}{\bot}{-}PCL_{28}{-}OH}$ and the diblock $\mathrm{Br{-}PS_{39}{-}\overset{\equiv}{\bot}{-}PCL_{28}{-}OH}$ was measured to be ~1.18 and ~1.12, respectively, indicating that both ROP and ATRP processes were well-controlled. Further substitution of each bromine end by an azide moiety resulted in the final precursor $\mathrm{N_3{-}PS_{39}{-}\overset{\equiv}{\bot}{-}PCL_{28}{-}N_3}$. It is well-known that the azidation reaction is extremely effective in polar solvent such as dimethylformamide (DMF) and typically completed within 24 h.[42,43] The successful substitution of the bromines is reflected in the strong N═N═N asymmetrical stretching vibration (~2100 cm^{-1}) (Figure 4). On the other hand, Figure 3 shows no obvious difference between the elution

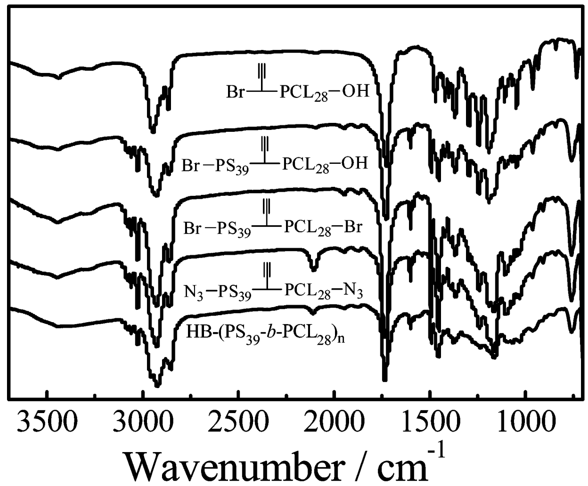

Figure 4. IR spectra of $\mathrm{Br{-}\overset{\equiv}{\bot}{-}PCL_{28}{-}OH}$, $\mathrm{Br{-}PS_{39}{-}\overset{\equiv}{\bot}{-}PCL_{28}{-}OH}$, $\mathrm{Br{-}PS_{39}{-}\overset{\equiv}{\bot}{-}PCL_{28}{-}Br}$, $\mathrm{N_3{-}PS_{39}{-}\overset{\equiv}{\bot}{-}PCL_{28}{-}N_3}$, and HB-($PS_{39}$-*b*-$PCL_{28}$)$_n$.

curves of $\mathrm{Br{-}PS_{39}{-}\overset{\equiv}{\bot}{-}PCL_{28}{-}OH}$ and $\mathrm{N_3{-}PS_{39}{-}\overset{\equiv}{\bot}{-}PCL_{28}{-}N_3}$, indicating no side reaction. In order to find how the PS subchain length and the overall chain molar mass affect the properties of such prepared hyperbranched copolymers HB-(PS-*b*-PCL)$_n$, we further made another diblock macromonomer ($\mathrm{N_3{-}PS_{18}{-}\overset{\equiv}{\bot}{-}PCL_{28}{-}N_3}$) with an identical PCL block but a shorter PS block. Its characterization results are summarized in Figure S1 of the Supporting Information.

The interchain "clicking" of $\mathrm{N_3{-}PS{-}\overset{\equiv}{\bot}{-}PCL{-}N_3}$ in DMF at 60 °C led to large hyperbranched copolymer chains HB-(PS-*b*-PCL)$_n$. Figure 5 (also Figures S2 and S3) lists the

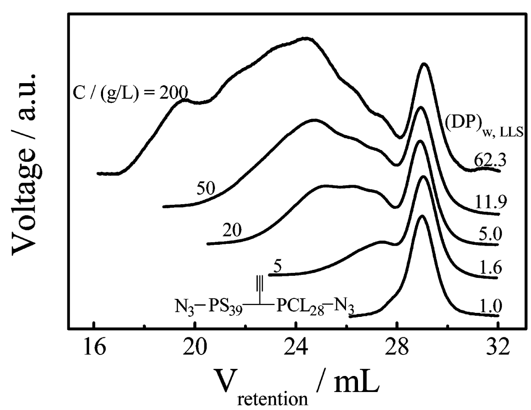

Figure 5. GPC curves of HB-(PS_{39}-*b*-PCL_{28})$_n$ monitored by RI detector, where the signed $(DP)_{w,LLS}$ values are calculated from the data collected by the MALLS detector.

characterization results. Note that the difference in the elution curves of HB-(PS-*b*-PCL)$_n$ measured by RI and MALLS detectors, as shown in Figure S2, is due to the fact that the signal from RI detector is proportional to the weight concentration of polymer, while that from MALLS detector is proportional to the weight concentration of polymer multiplied by the weight-average molar mass of polymer. It is known that GPC-RI is not able to effectively distinguish polymer chains with a similar hydrodynamic volume but different configurations.

Thus, we used absolute weight-average molar mass (M_w) of each hyperbranched copolymer determined by MALLS detector in current study. Furthermore, the self-polycondensation process is described in terms of the average degree of polycondensation (DP), where DP is defined as the number of macromonomers chemically coupled together inside each hyperbranched chain, i.e., $(DP)_w = M_{w,hyperbranched}/M_{w,macromonomer}$ and $(DP)_n = M_{n,hyperbranched}/M_{n,macromonomer}$, where $M_{w,hyperbranched}$ and $M_{w,macromonomer}$ are the weight-average molar mass of hyperbranched copolymers and macromonomers and $M_{n,hyperbranched}$ and $M_{n,macromonomer}$ are the number-average molar mass of hyperbranched copolymers and macromonomers, respectively. Hereafter, we will only use the weight-average degree of polycondensation [$(DP)_w$], instead of the number-average one [$(DP)_n$] to describe the self-polycondensation process.[21,22]

Figure 5 shows that the interchain "clicking" is promoted in a more concentrated precursor solution. GPC traces of HB-$(PS_{18}$-b-$PCL_{28})_n$ with a shorter PS block length are shown in Figure S4. Similar to our previous work on hyperbranched homopolystyrenes,[26] an obvious peak with a retention volume of 29.1 mL close to that of macromonomer precursor in the elution curve is observed in Figure 5 and Figure S4, presumably attributed to the unreacted macromonomer due to the incomplete functionality of the end group and/or high viscosity of polymer solutions in late stage of self-polycondensation. Moreover, this peak shifts to a higher retention volume by ~0.1 mL after polycondensation process when the concentration of the macromonomer is 200 g/L, indicating the occurrence of intramolecular cyclization. The molecular parameters of all HB-(PS-b-PCL)$_n$ measured by GPC are listed in Tables S1 and S2 in detail. There is no obvious difference of $(DP)_w$ between HB-$(PS_{39}$-b-$PCL_{28})_n$ and HB-$(PS_{18}$-b-$PCL_{28})_n$ chains for a given initial precursor concentration, indicating the PS block length does not affect the reactivity of the azide end group on the PS subchain. Both M_w/M_n and $(DP)_{w,MALLS}/(DP)_{w,RI}$ of such formed HB-$(PS_{39}$-b-$PCL_{28})_n$ chains increase significantly with the initial precursor concentration (Figure S3), similar to some previous results.[21−23] The successful "click" coupling of precursors N_3–PS(=)–PCL–N_3 is also reflected in a sharp decrease of the N=N=N asymmetric stretching vibration signal near ~2100 cm^{-1}, as shown in Figure 4.

It is well-known that the Mark−Houwink−Sakurada equation can be expressed as

$$[\eta] = KM_w^{\alpha} \quad (5)$$

where $[\eta]$, K, and M_w are the intrinsic viscosity, Mark−Houwink−Sakurada constant, and weight-average molar mass of a polymer, respectively. In principle, the Mark−Houwink−Sakurada parameter α can reflect the shape and compactness of polymers. More specifically, α is 0.2−0.5, 0.5, and 0.6−0.8 for branched polymers, linear polymers in theta solvents, and linear polymers in good solvents, respectively.[20,48] Note that for hyperbranched polymers each elution fraction out of GPC column contains polymer chains with a similar hydrodynamic volume but different topologic structures; thus, the parameter α for hyperbranched polymers is an average value. Previous results showed that the hyperbranched polystyrene chains have a self-similar property; namely, their size (R) and intrinsic viscosity ($[\eta]$) in toluene are scaled to their overall weight-average molar masses (M_w) and the weight-average subchain molar mass ($M_{w,s}$) as $R \sim M_w^{\gamma}M_{w,s}^{\varphi}$ with $\gamma = 0.47 \pm 0.01$ and $\varphi = 0.10 \pm 0.01$; $[\eta] \sim M_w^{\nu}M_{w,s}^{\mu}$ with $\nu = 0.39 \pm 0.01$ and $\mu = 0.31 \pm 0.01$.[25] The question here is whether a hyperbranched copolymer chain with two different and alternative subchains still keeps its self-similar character. Figure 6 shows the experimental result about such a $[\eta]-M_w$ relationship, where we also plot the $[\eta]-M_w$ relationships for linear PCL and PS (dashed lines) for comparison.[49,50] To the best of our knowledge, there is no theory to predict how $[\eta]$ is related to M_w for large hyperbranched copolymer chains in solutions up to now.

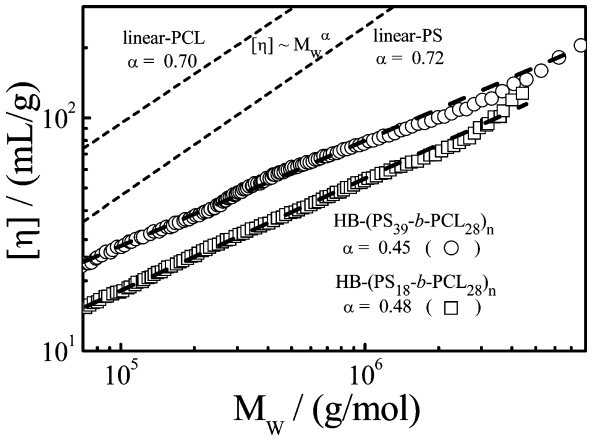

Figure 6. Weight-average molar masses (M_w) dependence of intrinsic viscosities ($[\eta]$) of HB-$(PS_{39}$-b-$PCL_{28})_n$ and HB-$(PS_{18}$-b-$PCL_{28})_n$ in THF. Dashed lines represent weight-average molar masses (M_w) dependence of intrinsic viscosities ($[\eta]$) of linear PCL and PS.

Figure 6 shows that for both HB-$(PS_{18}$-b-$PCL_{28})_n$ and HB-$(PS_{39}$-b-$PCL_{28})_n$ log[η] increases almost linearly with log M_w, indicating that their structures remains holding self-similar nature. The least-squares fittings result in $\nu = 0.48 \pm 0.01$ and 0.45 ± 0.01, respectively, for HB-$(PS_{18}$-b-$PCL_{28})_n$ and HB-$(PS_{39}$-b-$PCL_{28})_n$, much smaller than those for linear homopolymers, indicating a hyperbranched chain is more compact than its linear counterpart for a given overall molar mass. On the other hand, Figure 6 shows that $[\eta]$ of HB-$(PS_{18}$-b-$PCL_{28})_n$ is lower than that of HB-$(PS_{39}$-b-$PCL_{28})_n$ for a given M_w, which is attributed to their different branching densities because shorter subchains lead to a higher branching density. The corresponding scaling laws between the radius of gyration R_g and molar mass M_w for HB-$(PS_{39}$-b-$PCL_{28})_n$ and HB-$(PS_{18}$-b-$PCL_{28})_n$ are summarized in Figure S5. It is known that the scaling exponent between size and molar mass can also reflect the characteristic of shape and compactness of polymers. The power law exponents are 0.31 for HB-$(PS_{39}$-b-$PCL_{28})_n$ and 0.47 for HB-$(PS_{18}$-b-$PCL_{28})_n$, which are in accordance with the values of hyperbranched homopolymer PS and PCL,[25,51] indicating compact branched structure.

PCL can be used for biomedical applications because of its excellent biocompatibility and biodegradability. However, its crystallization has an impact on its degradation rate and affects its application. The architectural effect on properties of polymers has been studied by some groups,[5,52−56] including the architecture effect on the crystallization behavior of polymers containing PCL.[52−55] For example, Choi et al.[55] studied the crystallization of three hyperbranched PCLs as well as their linear counterparts with different lengths of homologous PCL segments and different numbers of branching points but similar molecular weights, and they found that the lengths of the linear backbone segments have a positive effect on the crystallization while the numbers of branching points bring opposite effect.

dx.doi.org/10.1021/ma501948g | Macromolecules 2014, 47, 8437−8445

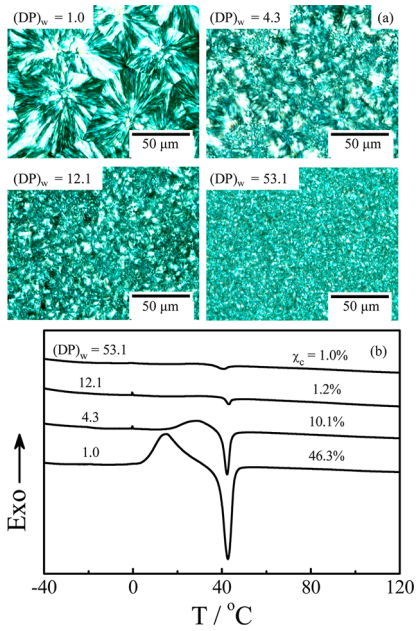

Figure 7. Crystalline properties of HB-$(PS_{18}$-*b*-$PCL_{28})_n$ with different $(DP)_w$s: (a) POM photos and (b) DSC curves (10 °C/min) during reheating.

Therefore, we further studied the crystallization of unfractionated HB-$(PS_{18}$-*b*-$PCL_{28})_n$ with different weight-average molar masses by POM and DSC measurements. Figure 7a shows how the size and shape of the crystalline domain of HB-$(PS_{18}$-*b*-$PCL_{28})_n$ change with its molar mass. For precursor $N_3{-}PS_{18}{\|}{-}PCL_{28}{-}N_3$ ($(DP)_w$ = 1.0), large integral spherocrystals were formed, while for large hyperbranched chains with $(DP)_w$ = 12.1, only few fragmentized crystals appeared; and for even larger hyperbranched chains with $(DP)_w$ = 53.1, no crystal was observed. The branching effect on the crystallization can be better viewed from the evolution of DSC curves (Figure 7b). The linear precursor $N_3{-}PS_{18}{\|}{-}PCL_{28}{-}N_3$ shows a broad crystallization peak at ~14 °C and a large melting peak at ~44 °C. The endothermic peak (the melting transition) at ~44 °C sharply decreases as the $(DP)_w$ increases, quantitatively reflecting in a decrease in the degree of crystallinity (χ_c) from 46.3% to 1.0%, which is similar to the results reported by Kawaguchi et al.[27] for hyperbranched PLA homopolymers. It is interesting to note that a broad exothermic peak attributed to the crystallization is still observable for HB-$(PS_{18}$-*b*-$PCL_{28})_n$ with $(DP)_w < 12.1$, but gradually shifts to a higher temperature as $(DP)_w$ increases. No exothermic peak can be detected when $(DP)_w \geq 12.1$, indicating the crystallization is completely prohibited due to the constraint of the branching topology. The observed melting transition temperature (T_m ~ 44 °C) is lower than that of the PCL homopolymer (~64 °C) but similar to those reported by Pan et al.[57] for linear PCL_{70}-*b*-PS_{24} diblock copolymer (~50 °C). Moreover, no glass transition of linear PS_{18} block is detected in both the heating and cooling processes, presumably because the short PS block has a low glass transition temperature (T_g) that is overlapped with the melting process of PCL.[57,58] In contrast, HB-$(PS_{39}$-*b*-$PCL_{28})_n$ with a longer PS block shows no crystallization in either DSC or POM even for the macromonomer $N_3{-}PS_{39}{\|}{-}PCL_{28}{-}N_3$ (Figure S6), revealing that besides using the branching effect, using a longer PS block can also completely suppress the crystallization of the PCL blocks inside, in consistent with the reported results in the literature.[59,60]

It is worth noting that the conclusions we drew above are established on polymer mixtures with broad polydispersity; as shown in Figure 5, we could draw a more quantitative conclusion with narrowly distributed hyperbranched polymers. Thus, the polydispersed HB-$(PS_{18}$-*b*-$PCL_{28})_n$ was further fractionated into a set of relatively narrowly distributed samples in a mixed solution of tetrahydrofuran/methanol. The GPC characterization of four selected fractions indicates that the polydispersity index ranges from 1.28 to 2.10, and the detailed characterization results are shown in Figure S7 and Table S3. Both POM and DSC measurements demonstrate that no obvious crystallization behavior was observed for all the fractions, even for the fraction with the smallest $(DP)_w$ ~ 6.0 (Figure 8),

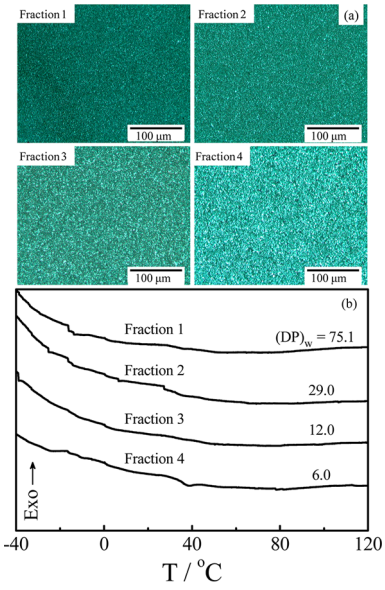

Figure 8. Crystalline properties of four HB-$(PS_{18}$-*b*-$PCL_{28})_n$ fractions with different $(DP)_w$s: (a) POM photos and (b) DSC curves (10 °C/min) during reheating.

indicating that the branching effect originated from only five times of interchain coupling is strong enough to completely suppress the crystallization of PCL blocks. In contrast, the crystallization can be still observed for unfractionated sample with $(DP)_w$ ~ 12, as shown in Figure 7. Such a discrepancy should be attributed to the existence of some crystallizable components such as linear macromonomers and dimers in the unfractionated mixtures, which also demonstrates that the preparation of narrowly distributed sample is the priority for further quantitative study of structure−property correlation. On the other hand, the complete restriction of crystallization of hyperbranched fraction with a low branching density ($(DP)_w$ ~ 6) is also due to the introduction of the uncrystallizable PS blocks because the crystallization of hyperbranched PCL homopolymer with a similar branching lengths but a much higher $(DP)_w$ was still observable in Choi's work.[55]

The above characterization demonstrates that the narrowly distributed hyperbranched fraction and macromonomer are uncrystallizable and crystallizable components in the unfractionated hyperbranched polymers, respectively. Therefore, it is meaningful to further get insight into the effect of one narrowly

dx.doi.org/10.1021/ma501948g | Macromolecules 2014, 47, 8437−8445

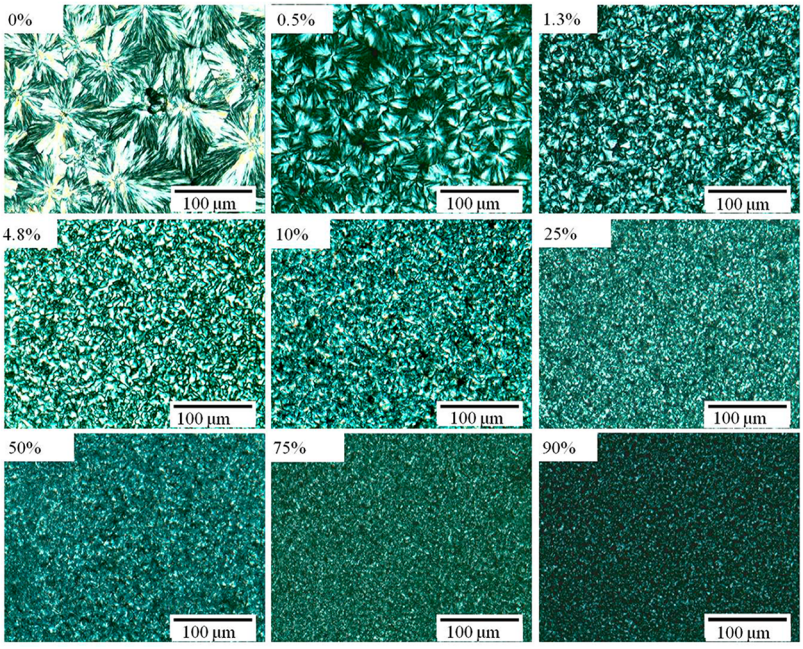

Figure 9. POM photos of polymer blends of HB-$(PS_{18}$-*b*-$PCL_{28})_{75.1}$ (fraction 1) and macromonomer $N_3-PS_{18}\!\!\parallel\!\!-PCL_{28}-N_3$ with different weight fractions (wt %) of HB-$(PS_{18}$-*b*-$PCL_{28})_{75.1}$.

distributed uncrystallizable hyperbranched fraction on the crystallization of the crystallizable linear macromonomer. Thus, polymer blends of macromonomer and hyperbranched fraction 1 [HB-$(PS_{18}$-*b*-$PCL_{28})_{75.1}$] with different weight fractions (wt %) were prepared for the POM and DSC measurements. Figure 9 shows that the size of the crystallization domain sharply decreases as the weight fraction of hyperbranched fraction 1 increases from 0 to 10%. When the weight fraction reaches 10%, only tiny fragmentized crystals, instead of integrated spherocrystals, were detected, indicating that the introduction of a small amount of uncrystallizable hyperbranched fraction is enough to significantly affect the crystallization morphology of the PCL blocks. The size of hyperbranched polymer in polymer blend film could be estimated by assuming that the size of hyperbranched polymer is similar to that in theta condition as polymer blend film can be treated as a concentrated polymer solution, in which hyperbranched polymer chains adopt ideal conformation. Considering the difference of the sizes of hyperbranched polymer between in a good solvent and in a theta solvent is small, the average viscometric size ($\langle R_\eta \rangle$) in a theta solvent (or in a polymer blend film) can be extracted from the famous Einstein viscosity relation, modeling the hydrated polymer molecules in terms of equivalent hydrodynamic spheres that would increase the viscosity to the same extent as solid spherical particles of volume V_e[25] in a good solvent, i.e.

$$[\eta] = 2.5N_A\left(\frac{V_e}{M_w}\right) \tag{6}$$

where $[\eta]$ and M_w are the intrinsic viscosity and weight-average molar mass of the hyperbranched polymer, respectively. Substituting $V_e = (4/3)\pi R_\eta^3$ into eq 6, we have

$$[\eta] = \frac{10\pi}{3}N_A\left(\frac{R_\eta^3}{M_w}\right) \quad \text{or} \quad R_\eta = \left(\frac{3[\eta]M_w}{10\pi N_A}\right)^{1/3} \tag{7}$$

Figure 6 shows that the average intrinsic viscosity of HB-$(PS_{18}$-*b*-$PCL_{28})_{75.1}$ in THF, a good solvent, is ~32 mL/g. Therefore, $\langle R_\eta \rangle$ of HB-$(PS_{18}$-*b*-$PCL_{28})_{75.1}$ is calculated to be ~13 nm. At a critical weight fraction of hyperbranched polymer (wt %), the whole volume of the blend is filled with hyperbranched polymers; wt % can be evaluated by using

$$\text{wt \%} = \frac{M_w}{\rho N_A \frac{4}{3}\pi\langle R_\eta \rangle^3} \tag{8}$$

where M_w, $\langle R_\eta \rangle$, ρ and N_A represent the weight-average molar mass, the average viscometric size of hyperbranched polymer, the density of the blend film, and Avogadro's number, respectively. Taking $M_w \sim 4.07 \times 10^5$ g/mol, $\langle R_\eta \rangle \sim 13$ nm, $\rho \sim 1.0$ g/mL and $N_A \sim 6.02 \times 10^{23}$ mol^{-1} into eq 8, wt % can be estimated as ~7.3%, indicating the hyperbranched polymers start to overlap at wt % ~ 7.3% in the blend film and to suppress the free spaces in which large spherulites can form, explaining why only tiny fragmentized crystals were observed when wt % is 10%.

The DSC melting traces of the blends with different weight fractions of HB-$(PS_{18}$-*b*-$PCL_{28})_{75.1}$ are shown in Figure 10. Figure 10a shows that all the melting peaks are located at the temperature range of 40−50 °C, and some of them contain two melting peaks, presumably due to the melting of the initial crystals grown during the cooling process and the melting of crystals grown during the heating process.[61] Figure 10b shows that the degree of crystallinity decreases as the weight fraction of hyperbranched fraction increases; namely, χ_c initially smoothly decreases from ~47% to ~21% as wt % increases from 0 to 67% and subsequently drops to 3.4% as wt % reaches to 75%. However, a linear decrease in χ_c with wt % is assumed to be observed if only dilution effect is considered, i.e., the dashed oblique line presented in Figure 10b, which is different from what we observed.

It is worth noting that the discrepancy between the transition wt % for the crystal size (wt % ~ 10%) and the degree of crystallinity (wt % ~ 67%) indicates that the crystal size can be

dx.doi.org/10.1021/ma501948g | *Macromolecules* 2014, 47, 8437−8445

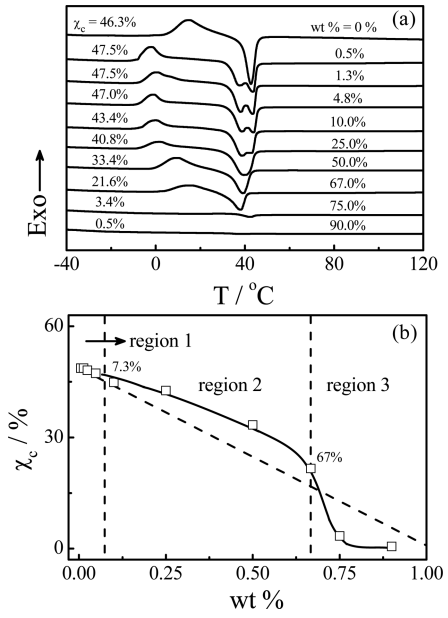

Figure 10. (a) DSC curves and (b) degree of crystallinity (χ_c) of polymer blends of HB-(PS_{18}-*b*-PCL_{28})$_{75.1}$ (fraction 1) and macromonomer $N_3-PS_{18}\|\!-PCL_{28}-N_3$ with different weight fractions (wt %) of HB-(PS_{18}-*b*-PCL_{28})$_{75.1}$ during reheating, where the scanning rate is 10 °C/min. The dashed oblique line presents the dilution effect of hyperbranched copolymer on the degree of crystallinity.

greatly regulated before a significant change of the overall degree of crystallinity. Combining the results of POM and DSC, the crystallization behavior of the polymer blend may contain three different regions: (1) In the first region (wt % < 7.3%), the hyperbranched polymer cannot fill all the polymer blend as wt % is lower than the critical weight fraction (7.3%), so spherulites can still form but the size of spherulites decreases with the increase in the wt % of the hyperbranched polymer while the degree of crystallinity just decreases slightly. (2) In the second region (7.3% < wt % < 67%), more spaces are occupied as wt % increases, but tiny fragmentized crystal can still form because there are abundant but small intrachain spaces for PCL chains to crystallize. (3) In the third region (wt % > 67%), no crystal is detected and the degree of crystallinity sharply decreases to minimum. Such a phenomenon was previously observed in some blend systems where the intercomponent interactions, such as hydrogen bonding[62] or dipole interaction,[63] were introduced into the blend system, which could be explained as the interaction was strong enough to enhance the miscibility of the two components to accordingly completely suppress the crystallization of the crystallizable component at a critical weight concentration. In our case, no specific interaction is assumed to exist between the two components with an identical chemical constituent but only configuration difference; therefore, we would like to attribute this trend to the extra restriction on the crystallization of macromonomer originated from the strong branching interaction of uncrystallizable hyperbranched chains when wt % is ~67%, at which the hyperbranched polymer chains are strongly interpenetrated with each other and result in a highly compact structure. In other words, the interpenetration eliminates all the free volume for the PCL chains to crystallize. This interesting result may provide some useful information for understanding the crystallization behavior of some other polymer blend systems.

CONCLUSION

In summary, we have developed an approach of combining ring-opening polymerization and atom transfer radical polymerization to construct model hyperbranched copolymers [HB-(PS-*b*-PCL)$_n$] with two kinds of controllable and long uniform subchains (PS and PCL) via a trifunctional initiator consisting of one alkyne, one hydroxyl, and one bromine group. Such prepared hyperbranched polymer has a self-similar structure with its intrinsic viscosity ([η]) scalable to its molar mass (M_w) as [η] ~ M_w^{ν}, where ν = 0.45 ± 0.01 for longer PS block and 0.48 ± 0.01 for shorter PS block. More importantly, we have explored the crystallization behavior of broadly and narrowly distributed HB-(PS-*b*-PCL)$_n$ copolymers. The results indicate both the crystal size and the degree of crystallinity can be significantly regulated by the PS subchain length and the overall polymerization degree. However, for a given $(DP)_w$, the crystallization behavior is much easier to be observed for polydispersed unfractionated samples due to the existence of the crystallizable low-molar-mass components. Finally, the study on the crystallization of polymer blends shows that the degree of crystallinity decreases dramatically when the weight fraction of hyperbranched fractions exceeds ~67%, implying some extra restriction exerted by hyperbranched fraction on the crystallization of the macromonomer. The discrepancy of the transition points of weight fraction between crystal size (~10%) and the degree of crystallinity (~67%) also indicates the crystal size can be greatly regulated before a significant change of the overall degree of crystallinity. It should be emphasized that our synthetic strategy can be applied to not only hydrophobic monomers but also hydrophilic monomers, e.g., methoxy poly(ethylene glycol) methacrylate (POEGMA) and (meth)acrylic acid (PMAA). Such hyperbranched structure may have more potential applications into many bio-related fields. The preparation of other hyperbranched copolymers made of different monomer categories is undergoing.

ASSOCIATED CONTENT

Supporting Information

^{1}H NMR spectra and GPC curves of macromonomer precursors $N_3-PS_{18}\|\!-PCL_{28}-N_3$, a comparison of $(DP)_{MALLS}$ and $(DP)_{RI}$ for HB-(PS_{18}-*b*-PCL_{28})$_n$ and HB-(PS_{39}-*b*-PCL_{28})$_n$, GPC curves of HB-(PS_{18}-*b*-PCL_{28})$_n$ with different $(DP)_w$, GPC curves of HB-(PS_{18}-*b*-PCL_{28})$_n$ fractions, POM and DSC studies of crystallization of HB-(PS_{39}-*b*-PCL_{28})$_n$, and GPC data for all the samples used. This material is available free of charge via the Internet at http://pubs.acs.org.

AUTHOR INFORMATION

Corresponding Authors

*E-mail llw@mail.ustc.edu.cn (L.L.).
*E-mail xdye@ustc.edu.cn (X.Y.).

Author Contributions

J.Y. and L.L. contributed equally to this work.

Notes

The authors declare no competing financial interest.

ACKNOWLEDGMENTS

The financial support of the Ministry of Science and Technology of China Key Project (2012CB933800), the National Natural Scientific Foundation of China Projects (51173177, 51273091 and 21274140), and the Hong Kong Special Administration Region

Earmarked Projects (CUHK4036/11P, 2130281/2060431; CUHK4035/12P, 2130306/4053005; and CUHK7/CRF/12G, 2390062) is gratefully acknowledged.

REFERENCES

(1) Choi, J.; Kwak, S. Y. *Macromolecules* **2003**, *36*, 8630.
(2) Unal, S.; Yilgor, I.; Sheth, J. P.; Wilkes, G. L.; Long, T. E. *Macromolecules* **2004**, *37*, 7081.
(3) Clarke, N.; De Luca, E.; Dodds, J. M.; Kimani, S. M.; Hutchings, L. R. *Eur. Polym. J.* **2008**, *44*, 665.
(4) Hutchings, L. R. *Soft Matter* **2008**, *4*, 2150.
(5) Hutchings, L. R.; Dodds, J. M.; Rees, D.; Kimani, S. M.; Wu, J. J.; Smith, E. *Macromolecules* **2009**, *42*, 8675.
(6) Konkolewicz, D.; Gray-Weale, A.; Perrier, S. *J. Am. Chem. Soc.* **2009**, *131*, 18075.
(7) Konkolewicz, D.; Poon, C. K.; Gray-Weale, A.; Perrier, S. *Chem. Commun.* **2011**, *47*, 239.
(8) Barbey, R.; Perrier, S. *Macromolecules* **2014**, *47*, 6697.
(9) Kong, L. Z.; Sun, M.; Qiao, H. M.; Pan, C. Y. *J. Polym. Sci., Part A: Polym. Chem.* **2010**, *48*, 454.
(10) Li, L. W.; Zhou, J. F.; Wu, C. *Macromolecules* **2012**, *45*, 9391.
(11) Dodds, J. M.; De Luca, E.; Hutchings, L. R.; Clarke, N. *J. Polym. Sci., Part B: Polym. Phys.* **2007**, *45*, 2762.
(12) Trollsås, M.; Hedrick, J. L.; Mecerreyes, D.; Dubois, P.; Jérôme, R.; Ihre, H.; Hult, A. *Macromolecules* **1998**, *31*, 2756.
(13) Trollsås, M.; Hedrick, J. L. *J. Am. Chem. Soc.* **1998**, *120*, 4644.
(14) Trollsås, M.; Hedrick, J. L. *Macromolecules* **1998**, *31*, 4390.
(15) Hedenqvist, M. S.; Yousefi, H.; Malmstrom, E.; Johansson, M.; Hult, A.; Gedde, U. W.; Trollsås, M.; Hedrick, J. L. *Polymer* **2000**, *41*, 1827.
(16) Heise, A.; Trollsås, M.; Magbitang, T.; Hedrick, J. L.; Frank, C. W.; Miller, R. D. *Macromolecules* **2001**, *34*, 2798.
(17) Emrick, T.; Chang, H. T.; Fréchet, J. M. J. *Macromolecules* **1999**, *32*, 6380.
(18) Oguz, C.; Unal, S.; Long, T. E.; Gallivan, M. A. *Macromolecules* **2007**, *40*, 6529.
(19) Unal, S.; Ozturk, G.; Sisson, K.; Long, T. E. *J. Polym. Sci., Part A: Polym. Chem.* **2008**, *46*, 6285.
(20) Kong, J.; Schmalz, T.; Motz, G.; Müller, A. H. E. *Macromolecules* **2011**, *44*, 1280.
(21) He, C.; Li, L. W.; He, W. D.; Jiang, W. X.; Wu, C. *Macromolecules* **2011**, *44*, 6233.
(22) Li, L. W.; He, C.; He, W. D.; Wu, C. *Macromolecules* **2011**, *50*, 8195.
(23) He, C.; He, W. D.; Li, L. W.; Jiang, W. X.; Tao, J.; Yang, J.; Chen, L.; Ge, X. S.; Chen, S. Q. *J. Polym. Sci., Part A: Polym. Chem.* **2012**, *44*, 3214.
(24) Li, L. W.; Wang, X.; Yang, J. X.; Ye, X. D.; Wu, C. *Macromolecules* **2014**, *47*, 650.
(25) Li, L. W.; Lu, Y. Y.; An, L. J.; Wu, C. *J. Chem. Phys.* **2013**, 114908.
(26) Li, L. W.; He, C.; He, W. D.; Wu, C. *Macromolecules* **2012**, *45*, 7583.
(27) Jikei, M.; Suzuki, M.; Itoh, K.; Matsumoto, K.; Saito, Y.; Kawaguchi, S. *Macromolecules* **2012**, *45*, 8237.
(28) Yoo, S. H.; Lee, J. H.; Lee, J. C.; Jho, J. Y. *Macromolecules* **2002**, *35*, 1146.
(29) Cheng, C.; Wooley, K. L.; Khoshdel, E. *J. Polym. Sci., Part A: Polym. Chem.* **2005**, *43*, 4754.
(30) Li, Y. T.; Armes, S. P. *Macromolecules* **2005**, *38*, 8155.
(31) Hong, H. Y.; Mai, Y. Y.; Zhou, Y. F.; Yan, D. Y.; Cui, J. *Macromol. Rapid Commun.* **2007**, *28*, 591.
(32) Wei, H.; Wu, D. Q.; Li, Q.; Chang, C.; Zhou, J. Q.; Zhang, X. Z.; Zhuo, R. X. *J. Phys. Chem. C* **2008**, *112*, 15329.
(33) Zhou, Y.; Huang, W.; Liu, J.; Zhu, X.; Yan, D. *Adv. Mater.* **2010**, *22*, 4567.
(34) Lin, S. L.; Zhu, W. J.; He, X. H.; Xing, Y. H.; Liang, L. Y.; Chen, T.; Lin, J. P. *J. Phys. Chem. B* **2013**, *117*, 2586.
(35) Vyhnalkova, R.; Eisenberg, A.; van de Ven, T. G. M. *Langmuir* **2011**, *27*, 11296.
(36) Chen, S.; Zhang, X. Z.; Cheng, S. X.; Zhuo, R. X.; Gu, Z. W. *Biomacromolecules* **2008**, *9*, 2578.
(37) Prabaharan, M.; Grailer, J. J.; Pilla, S.; Steeber, D. A.; Gong, S. *Biomaterials* **2009**, *30*, 3009.
(38) Hu, J. M.; Qian, Y. F.; Wang, X. F.; Liu, T.; Liu, S. Y. *Langmuir* **2012**, *28*, 2073.
(39) Jones, M. C.; Gao, H.; Leroux, J. C. *J. Controlled Release* **2008**, *132*, 208.
(40) Simon, P. F. W.; Müller, A. H. E.; Pakula, T. *Macromolecules* **2001**, *34*, 1677.
(41) Kainthan, R. K.; Muliawan, E. B.; Hatzikiriakos, S. G.; Brooks, D. E. *Macromolecules* **2006**, *39*, 7708.
(42) Binder, W. H.; Sachsenhofer, R. *Macromol. Rapid Commun.* **2007**, *28*, 15.
(43) Binder, W. H.; Sachsenhofer, R. *Macromol. Rapid Commun.* **2008**, *29*, 952.
(44) Lodge, T. P. *Macromolecules* **2009**, *42*, 3827.
(45) Nojima, S.; Fujimoto, M.; Kakihira, H.; Sasaki, S. *Polym. J.* **1998**, *30*, 968.
(46) Shi, G. Y.; Yang, L. P.; Pan, C. Y. *J. Polym. Sci., Part A: Polym. Chem.* **2008**, *46*, 6496.
(47) Gungor, E.; Durmaz, H.; Hizal, G.; Tunca, U. *J. Polym. Sci., Part A: Polym. Chem.* **2008**, *46*, 4459.
(48) Mori, H.; Müller, A. H. E.; Simon, P. F. W. In *Macromolecular Engineering: Precise Synthesis, Materials, Properties, Applications*; Matyjaszewski, K., Gnanou, Y., Leibler, L., Eds.; Wiley-VCH: Weinheim, 2007; Vol. 2, p 973.
(49) Brandrup, J.; Immergut, E. H.; Grulke, E. A. *Polymer Handbook*, 4th ed.; John Wiley & Sons, Inc.: New York, 1999; Chapter 7, p 68.
(50) Huang, Y.; Xu, Z. D.; Huang, Y. P.; Ma, D. Z.; Yang, J. C.; Mays, J. W. *Int. J. Polym. Anal. Charact.* **2003**, *8*, 383.
(51) Yang, H. J.; Xu, J. B.; Pispas, S.; Zhang, G. Z. *RSC Adv.* **2013**, *3*, 6853.
(52) Trollsås, M.; Atthof, B.; Würsch, A.; Hedrick, J. L.; Pople, J. A.; Gast, A. P. *Macromolecules* **2000**, *33*, 6423.
(53) Skaria, S.; Smet, M.; Frey, H. *Macromol. Rapid Commun.* **2002**, *23*, 292.
(54) Stancik, C. M.; Pople, J. A.; Trollsås, M.; Lindner, P.; Hedrick, J. L.; Gast, A. P. *Macromolecules* **2003**, *36*, 5765.
(55) Choi, J.; Kwak, S. Y. *Macromolecules* **2004**, *37*, 3745.
(56) Kandadai, M. A.; Anumolu, R.; Wang, X.; Baskaran, D.; Pease, L. F., III; Bedrov, D.; Smith, G. D.; Mays, J. W.; Magda, J. J. *Eur. Polym. J.* **2011**, *47*, 2022.
(57) Shi, G. Y.; Sun, J. T.; Pan, C. Y. *Macromol. Chem. Phys.* **2011**, *212*, 1305.
(58) O'Driscoll, K.; Sanayei, R. A. *Macromolecules* **1991**, *24*, 4479.
(59) Heuschen, J.; Jérôme, R.; Teyssié, P. *J. Polym. Sci., Part B: Polym. Phys.* **1989**, *27*, 523.
(60) Zhao, Y. F.; Fan, X. H.; Chen, X. F.; Wan, X. H.; Zhou, Q. F. *Polymer* **2005**, *46*, 5396.
(61) Nunez, E.; Ferrando, C.; Malmstrom, E.; Claesson, H.; Werner, P. E.; Gedde, U. W. *Polymer* **2004**, *11*, 5251.
(62) Kuo, S. W.; Huang, W. J.; Huang, C. F.; Chan, S. C.; Chang, F. C. *Macromolecules* **2004**, *37*, 4164.
(63) Plivelic, T. S.; Cassu, S. N.; do Carmo Goncalves, M.; Torriani, I. L. *Macromolecules* **2007**, *40*, 253.

NOTE ADDED AFTER ASAP PUBLICATION

This article posted asap on November 17, 2014. The first two sentences of the abstract have been revised. The correct version posted on November 25, 2014.